Biomaterials Science

ROYAL SOCIETY OF CHEMISTRY

PAPER

View Article Online
View Journal | View Issue

Cite this: *Biomater. Sci.*, 2023, **11**, 2738

Immunogenicity assessment of swim bladder-derived biomaterials†

Yuanyuan Kong,‡[a] Jing Liu,‡[a] Honghui Jiang,[a] Lili Song,[a,c] Deling Kong [a,b] and Zhihong Wang *[a]

Fish swim bladder-derived biomaterials are prospective cardiovascular materials due to anti-calcification, adequate mechanical properties, and good biocompatibility. However, their immunogenic safety profile, which primarily determines their feasibility as medical devices in clinical practice, remains unknown. Herein, the immunogenicity of glutaraldehyde crosslinked fish swim bladder (Bladder-GA) and un-cross-linked swim bladder (Bladder-UN) samples was examined using *in vitro* and *in vivo* assays according to ISO 10993-20. The *in vitro* splenocyte proliferation assay showed that cell growth was lower in the extract medium of Bladder-UN and Bladder-GA, compared to the LPS-or Con A-treated group. Similar results were obtained in *in vivo* assays. In the subcutaneous implantation model, the thymus coefficient, spleen coefficient and ratio of immune cell subtypes showed no significant difference between the bladder groups and the sham group. In terms of the humoral immune response, the total IgM concentration was lower in the Bladder-GA and Bladder-UN groups (988 ± 238 μg ml^{-1} and 1095 ± 296 μg ml^{-1}, respectively) than that in the sham group (1329 ± 132 μg ml^{-1}) at 7 days. The total IgG concentrations were 422 ± 78 μg ml^{-1} in Bladder-GA and 469 ± 172 μg ml^{-1} in Bladder-UN at 30 days, which were slightly higher than that in the sham group (276 ± 95 μg ml^{-1}) but there was no significant difference compared with Bovine-GA (468 ± 172 μg ml^{-1}), indicating that these materials did not elicit a strong humoral immune response. Systemic immune response-related cytokines and C-reactive protein were stable during implantation, while IL-4 levels increased with time. The classical foreign body response was not observed around all the implants, and the ratio of CD163+/iNOS macrophages in Bladder-GA and Bladder-UN was higher than that in the Bovine-GA group at the implanted site at 7 and 30 days. Finally, no organ toxicity was observed in any of the groups. Collectively, the swim bladder-derived material did not elicit significant aberrant immune responses *in vivo*, giving strong confidence for its application in tissue engineering or medical devices. Furthermore, more dedicated research on immunogenic safety assessment in large animal models is encouraged to facilitate the clinical practice of swim bladder-derived materials.

Received 1st September 2022,
Accepted 17th January 2023

DOI: 10.1039/d2bm01419j

rsc.li/biomaterials-science

1. Introduction

With the development of longevity and aging societies worldwide, the incidence of valvular heart disease (VHD) has been increasing in recent years and has attracted extensive attention. Approximately 13.3% of elderly patients suffer from VHD.[1] Globally, there are more than 300 000 heart valve replacement surgeries each year,[2] and this number is expected to triple by 2050.[3] Bioprosthetic heart valves (BHVs) are popular for elderly patients because of their good biocompatibility and no requirement of anticoagulant treatment. BHVs are made entirely or partially from animal-derived materials. Currently, bovine pericardium and porcine aortic valves are the main substitutes that are treated using special chemical or physical methods to remove immunogenicity, and glutaraldehyde-crosslinking is used to improve durability and reduce the antigenicity of valves.[4] In recent years, transcatheter aortic valve replacement (TAVR) has been widely used in elderly patients.[5] The safety and durability of bioprosthetic heart valves are of pivotal concern. As reported, the lifespan is usually approximately 10–15 years for surgical heart valves and 8–10 years for TAVR devices.[6] The types of bioprosthetic heart valve failure can be divided into structural degeneration (calcification, tear, fibrosis, and failure), non-structural degener-

[a]*Tianjin Key Laboratory of Biomaterial Research, Institute of Biomedical Engineering, Chinese Academy of Medical Sciences and Peking Union Medical College, Tianjin 300192, China. E-mail: wangzhihong@bme.pumc.edu.cn*
[b]*Key Laboratory of Bioactive Materials of Ministry of Education, State Key Laboratory of Medicinal Chemical Biology, College of Life Science, Nankai University, Tianjin 300071, China*
[c]*College of Life Sciences, Tiangong University, Tianjin 300387, China*
†Electronic supplementary information (ESI) available. See DOI: https://doi.org/10.1039/d2bm01419j
‡These authors contribute equally to this work.

ation (pannus), thrombosis, and endocarditis. Among them, calcification is one of the main causes of valve degeneration and may lead to stenosis or dysfunction of bioprosthetic heart valves, ultimately limiting their long-term use as biological valves.[7]

Due to their superior anti-calcification property,[8,9] swim bladder-derived materials have attracted considerable attention and interest from academics and industries in the field of cardiovascular research. The mechanical properties, blood compatibility, and biocompatibility for use as cardiovascular materials have been proven by *in vitro* assays.[8] In addition, several types of cardiovascular biomaterials and devices made from swim bladders have been developed, such as heart valves, small-diameter vascular grafts (SDVGs), and vascular patches. A novel TAVR device with glutaraldehyde-crosslinked carp swim bladders as heart valvular leaflets was successfully prepared and it exhibited excellent anti-calcification ability, rapid endothelialization, and good hemodynamic properties in a sheep lung valve replacement model.[10] In our previous work, a vascular graft with a chemically crosslinked swim bladder by the rolling method was developed, and further, rat abdominal artery replacement *in situ* assessment confirmed its good patency and neo-tissue regeneration at 1 month after implantation.[8] Similar results were obtained in another study in which a vascular patch was developed by coating rapamycin on decellularized goldfish swim bladder samples and exhibited low neointimal thickness formation and macrophage infiltration.[11] These studies suggest that swim bladders have great potential as new substitutes for cardiovascular biomaterials. Moreover, the interest in developing swim bladders for other biomedical applications is increasing.[12,13] These studies are encouraging, but many issues still need to be clarified before their application.

Similar to other animal-derived materials, the immunogenic safety of fish-swim bladder-derived biomaterials is a major concern. According to clinical investigations, immune rejection by the body of the biomaterial is the main cause resulting in the ultimate failure of xenografts. Recent studies have verified that the immunogenicity of animal-derived materials can induce calcification. Immune cells, such as lymphocytes and macrophages, which secrete numerous cytokines, are speculated to be related to early calcification in young patients during transplantation and ultimately lead to the failure of transplantation.[14] Meanwhile, the carbohydrate epitope α-1,3-galactose (α-gal) is the main antigen that causes xenotransplantation rejection in non-primate animals, such as pigs and cattle.[15] In addition, non-gal antigens, such as *N*-glycolylneuraminic acid (Neu5Gc), also play a vital role in xenograft rejection in humans (but non-human primates).[16] Thus, comprehensive studies on the immunogenicity of new materials are essential to provide important information and help researchers and clinicians predict their clinical outcomes.

In the present study, the immunogenicity of the fish swim bladder crosslinked with glutaraldehyde (Bladder-GA) and uncrosslinked fish swim bladder (Bladder-UN) was verified by *in vitro* and *in vivo* experiments according to ISO10993-20.[17] Based on previous exploration of swim bladder-derived cardiovascular biomaterials, we found that the swim bladder of silver carp exhibits low calcification, adequate mechanical properties, high stability, good hemocompatibility, and cytocompatibility.[9] Therefore, we chose silver carp swim bladders as the research object in this study. We carefully examined the immune responses between the body and the swim bladder. In particular, lymphocyte proliferation assay and mass coefficient changes of immune organs were used to assess the effect of swim bladders on lymphocyte function. The systemic immune response was assessed by observing the changes in immune cells in the peripheral blood and spleen, as well as by monitoring the variation in C-reaction proteins and other related cytokines. Importantly, serum IgG and IgM levels were measured to verify the humoral immune reaction using enzyme-linked immunosorbent assay (ELISA) at 30 days after implantation. Furthermore, the local immune response to the swim bladder was evaluated by assessing M1/M2 macrophage phenotypes using immunohistochemical staining. Finally, the histopathology of the main organs was assessed by H&E and TUNEL staining.

2. Materials and methods

2.1 Materials

Antibodies including anti-iNOS (ab283655) and anti-CD163 (ab182422) were purchased from Abcam (USA). Mouse-anti-CD45 (103108), mouse-anti-CD4 (100408), mouse-anti-CD8 (100732), mouse-anti-CD19 (152407), and cell staining buffer (420201) were purchased from BioLegend (USA). 4,6-Diamidino-2-phenylindole (DAPI) was obtained from Southernbiotech (USA). 4% Paraformaldehyde and a DAB substrate kit (DA1010) were purchased from Solarbio Company (Beijing, China). Male Balb/c mice (8 weeks) were obtained from Charles River Company (Beijing, China). Cell counting kit-8 (CK04) was obtained from Dojindo Company (Japan). A mouse IgG ELISA kit (EMC116) and a mouse IgM ELISA kit (EMC129) were purchased from Neobioscience Company (Shenzhen, China). An ELISA kit for C reactive protein (CRP) was purchased from Cloud Clone Company (Wuhan, China). HRP-labeled goat anti-rabbit IgG (A0208) and a TUNEL kit were obtained from Beyotime Company (Shanghai, China). All animal procedures were performed in accordance with the Guidelines for Care and Use of Laboratory Animals of Nankai University and approved by the Center of Tianjin Animal Experiment Ethics Committee and Authority for Animal Protection.

2.2 Preparation of the three types of valve materials

The adipose tissue on the surfaces of the swim bladder and bovine pericardium was removed and washed in sterile phosphate buffer (PBS, PH = 7.4). The tissues were then decellularized through a series of procedures. First, they were treated with 1% sodium dodecyl sulfate (SDS) solution and 1% TritonX-100 solution (Solarbio, China) at room temperature

with gentle shaking. After cleaning with PBS solution several times, deoxyribonuclease (DNase, Sigma) and ribonuclease (RNase, Sigma, US) were incubated overnight at 37 °C. Next, the acellular fish swim bladder and bovine pericardium were crosslinked with 0.625% glutaraldehyde (GA) at room temperature for 12 h and 48 h. The crosslinked materials were stored in physiological saline containing 2% penicillin–streptomycin solution at 4 °C.

2.3 Splenocyte proliferation assay *in vitro*

Spleen cells were isolated from mouse spleen. Cervical vertebral dissociation was used to sacrifice the mice, which were then immersed in 75% ethanol for sterilization. The spleen was cut into pieces, triturated with a syringe piston, and then filtered through a 70 μm filter to remove cells on the clean bench. After centrifugation at 1500 rpm for 5 min, the supernatant was discarded. The red blood cells were disrupted in 3 ml of erythrocyte lysate at 4 °C for 3 min and terminated with 4 ml of 1640 culture medium (Gibco, US) containing 10% fetal bovine serum (FBS, Gibco, US) and 1% penicillin–streptomycin solution (Solarbio, China). The cells were washed twice to obtain a single-cell suspension.

For preparation of the material extract, first, the fish bladder material crosslinked with glutaraldehyde and the uncrosslinked fish bladder material were cut into 1 × 1 cm sheets, immersed in 75% ethanol, and irradiated under a UV lamp for 8 h. Then, the materials (1 × 1 cm, n = 6) were immersed in 2 ml of 1640 medium and extracted for 24 h at 37 °C. The extract of materials was obtained using a 0.22 μm filtration membrane.

The spleen cells were cultured respectively in 1640 culture medium and extracts of two groups of samples, and inoculated into 96-well plates with 4×10^5 cells, and 6 parallel wells were set for each group. Lipopolysaccharide (LPS, Sigma, 100 ng ml^{-1}) and concanavalin A (ConA, Sigma, 5 μg ml^{-1}) were used as positive controls. After 1 and 3 days, cell counting kit-8 (CCK-8) reagent was added. The absorbance was measured at 450 nm under a microplate reader.

2.4 Establishing the subcutaneous implantation model of mice

After the adaptation period, the mice were weighed and randomly divided into the sham operation group (Sham), GA-crosslinked swim bladder group (Bladder-GA), non-crosslinked swim bladder group (Bladder-UN) and GA-crosslinked bovine pericardium group (Bovine-GA), with 6 mice in each group. 4% chloral hydrate was used for anesthesia preparation and a 1 cm incision was made in the back. Biological materials (1 × 1 cm) were implanted and sutured respectively in Bladder-GA, Bladder-UN and Bovine-GA groups, while the sham group was sutured directly. The positive control was constructed with 0.12 ml of equal volume mixture of complete Freund's adjuvant (CFA) and bovine serum albumin (BSA, 3.3 g l^{-1}) at 1, 8, 15 and 22 days. After implantation, the postoperative status and weight changes were recorded. The samples were taken at 3, 7 and 30 days after surgery. Mouse eyeballs were extracted with elbow tweezers, and part of the blood was collected for blood routine examination and the rest of the blood was kept for 2 h and centrifuged at 3500 rpm for 10 min to obtain serum, which was stored at −80 °C for the detection of cytokines, C-reactive protein and immunoglobulin. After sacrificing the mice, they were soaked in 75% ethanol for several minutes, then the abdominal cavity and back were cut open, and the implanted materials were removed for pathology and immunofluorescence staining. The spleen and thymus were removed aseptically and their weights were recorded for the calculation of the mass coefficient of immune organs (the thymus coefficient = thymus weight/body weight; spleen coefficient = spleen weight/body weight). Later, the spleen was used to extract cells. The heart, liver, kidneys and lungs were removed and stored in 4% paraformaldehyde solution for pathological examination.

2.5 Splenocyte proliferation assay *in vivo*

At 7 and 30 days after subcutaneous implantation, spleen samples were extracted from mice to prepare spleen single-cell suspensions using the methods described in section 2.3. The spleen cells were inoculated into 96 well plates with 4×10^5 cells, 200 μl per well, and 6 parallel wells were set for each animal. After 72 h, the CCK-8 reagent was added. The absorbance was measured at 450 nm under the microplate reader.

2.6 Detection of lymphocyte subtypes

The spleen samples of mice implanted for 7 and 30 days were extracted to prepare spleen single-cell suspensions using the methods described in section 2.3. Mouse anti-CD45, anti-CD3, anti-CD19, anti-CD4, and anti-CD8 antibodies were labeled into each flow tube. The tubes were treated with an antibody mixture containing 100 μl of cell staining buffer and antibodies, and incubated for 0.5 h in the dark. Then the tubes were washed twice with PBS solution and centrifuged at 3500 rpm. Finally, 500 μl of 4% paraformaldehyde-fixed solution was added to each tube before flow cytometry (BD Biosciences, USA) testing.

2.7 Serum immunoglobulin, C-reactive protein and cytokine

Mouse serum total IgG, IgM and C-reactive protein were measured using the corresponding ELISA kits, and the serum concentrations of cytokines were determined using Luminex technology by Univ-bio company.

2.8 Histopathological staining

The heart, liver, lungs, kidneys and thymus of the mice were dehydrated, transparent and embedded. The tissues were cut into paraffin blocks and sections with a thickness of 0.6 μm. The materials at the implanted site were dehydrated in 30% sucrose solution, and then transferred into an optimal cutting temperature compound (OCT, Sakura, Japan), and rapidly frozen at −20 °C. Then 0.6 μm frozen sections were prepared using the freezing section mechanism. After staining with hematoxylin & eosin (H&E, Leagene, China), inflammatory reactions and pathological changes of various organs and the

implanted site were observed under a microscope (Olympus, BX53).

2.9 Immunohistochemical staining

The implanted material was cut into 0.6 μm thickness by frozen sections and stained with iNOS representing M1 macrophages and CD163 representing M2 macrophages. Firstly, the sections were cleaned with PBS for 5 min. Before labeling with iNOS, the sections were broken with 0.1% TritonX-100 and cleaned with PBS three times. Then they were sealed with a peroxidase blocker for 10 min and cleaned three times for 5 min each and then the 5% BSA solution was closed for 30 min and we discarded the excess liquid before primary antibody incubation. The primary antibody (iNOS, 1: 50, CD163, 1: 200) was incubated overnight at 4 °C, and then cleaned with PBS three times. The secondary antibody HRP-labeled goat anti-rabbit IgG (1:50) was incubated at room temperature for 2 h and washed with PBS three times. The DAB substrate kit (50 μl liquid A + 50 μl liquid B + 900 μl PBS solution) was used for chromogenic (3–10 min) detection, and cleaned 3 times. Then the hematoxylin was dyed for 3 min and rinsed with water for 3 min. The sections were immersed in 95% ethanol and 100% ethanol for 2 min each and then sliced into xylene solution twice, 3 min each time. After drying, the sections were observed under an immunofluorescence microscope.

2.10 Statistical analysis

The results are shown as mean ± standard deviation (s.d). One-way analysis of variance (ANOVA) was performed for statistical analysis of the data. Statistical significance was set at $P < 0.5$.

3. Results

3.1 Splenocyte proliferation *in vitro* and *in vivo*

Splenocytes were cultured in the extracts of Bladder-GA and Bladder-UN for 1 and 3 days. The absorbance values of Bladder-GA (0.77 ± 0.02) and Bladder-UN (0.05 ± 0.01) indicated no difference compared with that of the untreated group (0.10 ± 0.03) at 450 nm at 1 day and these values were significantly lower than those of LPS (0.14 ± 0.05) and ConA (0.36 ± 0.10) (Fig. 1A). The values of Bladder-GA (0.04 ± 0.01) and Bladder-UN (0.02 ± 0.01) groups were lower than that of the untreated group (0.06 ± 0.01) at 3 days (Fig. 1B). For the subcutaneous implant model, splenocytes were cultured *in vitro* for 72 h and their OD values were measured at 450 nm. The OD values of the sham, Bladder-GA and Bladder-UN groups were 1.40 ± 0.13, 0.49 ± 0.09 and 0.63 ± 0.15 after 7 days, and 0.43 ± 0.08, 0.39 ± 0.06 and 0.20 ± 0.03 after 30 days. The OD values of Bladder-GA and Bladder-UN groups were both lower than those of the sham group at 7 days (Fig. 1C). There was no significant difference between the Bladder-GA and sham groups at 30 days (Fig. 1D).

3.2 Changes of the body weight, thymus coefficient and spleen coefficient of mice

The changes in mouse body weight during subcutaneous implantation were recorded, and the overall weight change was relatively stable, except for a slight decrease for a short term after surgery. At the end of 30 days of subcutaneous implantation, a significant increase was observed, indicating that the mice were growing well (Fig. 2A).

The thymus and spleen coefficients of mice are commonly used to study the effects of materials on the immune organs. There is no obvious change in the thymus coefficient for both 7 days or 30 days, Bladder-GA (1.70 ± 0.47 mg g^{-1}, 1.48 ± 0.13 mg g^{-1}), Bladder-UN (1.61 ± 0.13 mg g^{-1}, 1.57 ± 0.10 mg g^{-1}), and Bovine-GA (1.61 ± 0.13 mg g^{-1}, 1.60 ± 0.12 mg g^{-1}) groups had no significant difference compared with the sham group (1.70 ± 0.30 mg g^{-1}, 1.69 ± 0.15 mg g^{-1}). No significant difference was observed between the two time points (Fig. 2B). The spleen coefficient of the sham, Bladder-GA, Bladder-UN, and Bovine-GA groups are 4.31 ± 0.54 mg g^{-1}, 4.49 ± 0.95 mg g^{-1}, 4.90 ± 0.53 mg g^{-1}, and 5.46 ± 0.53 mg g^{-1} for 7 days, and 4.32 ± 0.26 mg g^{-1}, 4.46 ± 0.57 mg g^{-1}, 3.92 ± 0.31 mg g^{-1}, and 4.25 ± 0.61 mg g^{-1} for 30 days. The spleen coefficient results were consistent with the thymus coefficient results (Fig. 2C).

3.3 Serum immunoglobulin detection

We detected serum IgM and IgG levels at 7 and 30 days after subcutaneous implantation. The serum total IgM concentrations of mice in the Bladder-GA (988 ± 238 μg ml^{-1}) and Bladder-UN (1095 ± 296 μg ml^{-1}) groups were slightly lower than those in the sham group (1329 ± 132 μg ml^{-1}) at 7 days, and there was little difference between the two groups. It could be seen that the serum total IgG concentration of mice in the Bladder-GA (422 ± 78 μg ml^{-1}) and Bladder-UN (469 ± 172 μg ml^{-1}) groups were slightly higher than those in the sham group (276 ± 95 μg ml^{-1}), but similar to that in the Bovine-GA group (468 ± 172 μg ml^{-1}) at 30 days, with no significant difference (Fig. 3).

3.4 The subtypes of splenocytes

Subtype analysis of splenocytes of mice implanted subcutaneously for 7 days and 30 days showed that the proportion of CD19+ and CD3+ cells in the Bladder-GA, Bladder-UN, Bovine-GA, and BSA + CFA groups was not significantly different from that in the sham group after subcutaneous implantation for 7 days. The proportions of CD3+CD8+ and CD3+CD4+ cells were similar to those in the sham group. After 30 days, there was no significant difference in the proportion of CD19+ and CD3+CD8+ cells in the Bladder-GA, Bladder-UN, Bovine-GA, and BSA + CFA groups compared with the sham group. The proportion of CD3+ and CD3+CD4+ cells in the BSA + CFA group was lower than that in the sham group, and there was hardly any significant difference in the proportion of CD3+ and CD3+CD4+ cells in the Bladder-GA, Bladder-UN, and Bovine-GA groups compared with the sham group (Fig. 4).

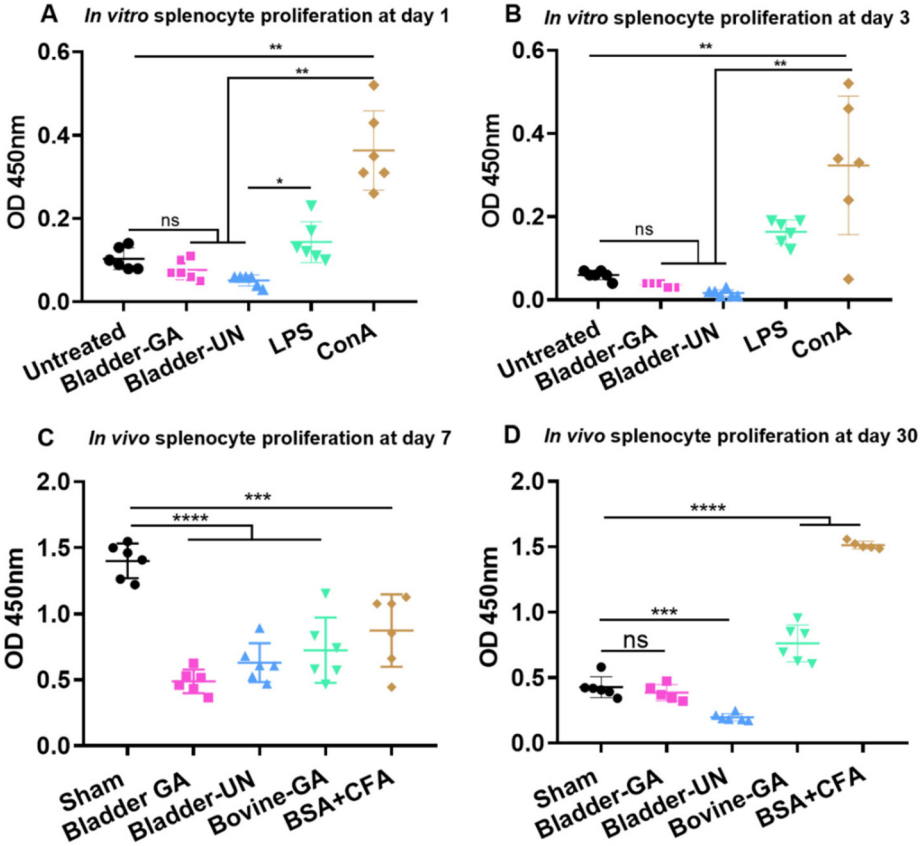

Fig. 1 The splenocyte proliferation *in vitro* at day 1 (A) and day 3 (B), $n = 6$. Meanwhile, the splenocyte proliferation in 5 groups was exhibited after implantation at 7 days (C) and 30 days (D), $n = 6$. $^{**}p < 0.01$, $^{***}p < 0.001$, $^{****}p < 0.0001$, ns = non-significant.

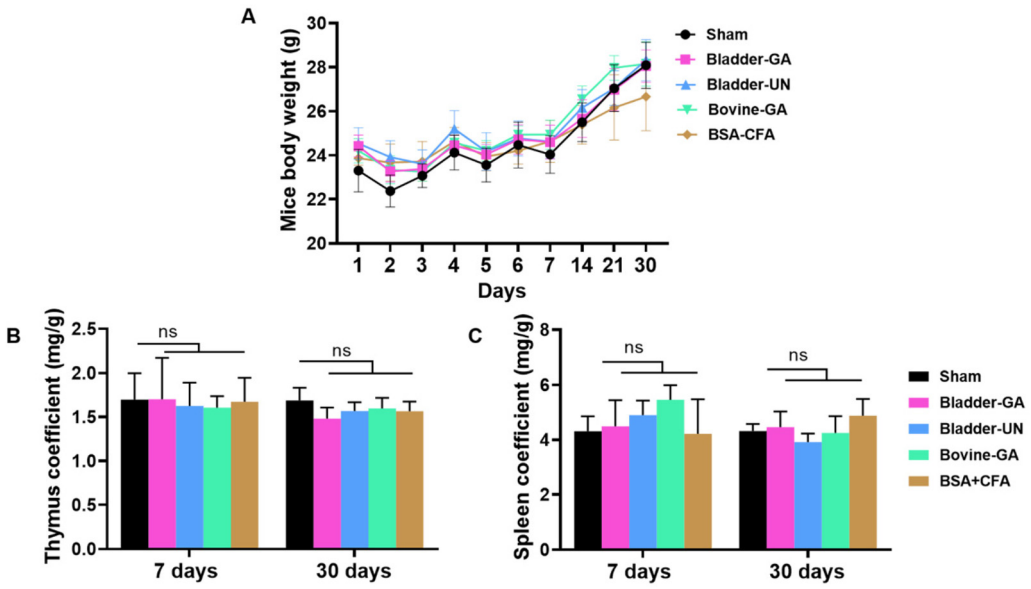

Fig. 2 Changes of body weight, thymus coefficient and spleen coefficient of mice. During the 30 days of implantation, the body weight increased (A). The thymus coefficients at 7 days and 30 days after subcutaneous implantation were basically the same among the five groups (B). The spleen coefficients and the thymus coefficient were similar in all groups at 7 and 30 days (C). ns = non-significant, $n = 6$.

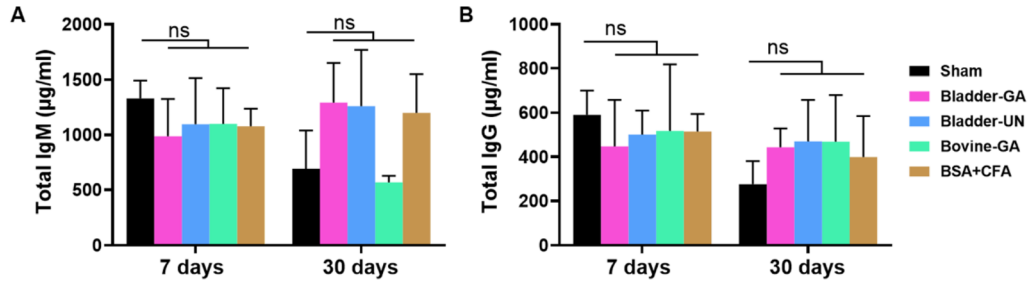

Fig. 3 The total IgM (A) and IgG (B) concentration in the serum of mice at 7 and 30 days in 5 groups after subcutaneous implantation. ns = non-significant, n = 4.

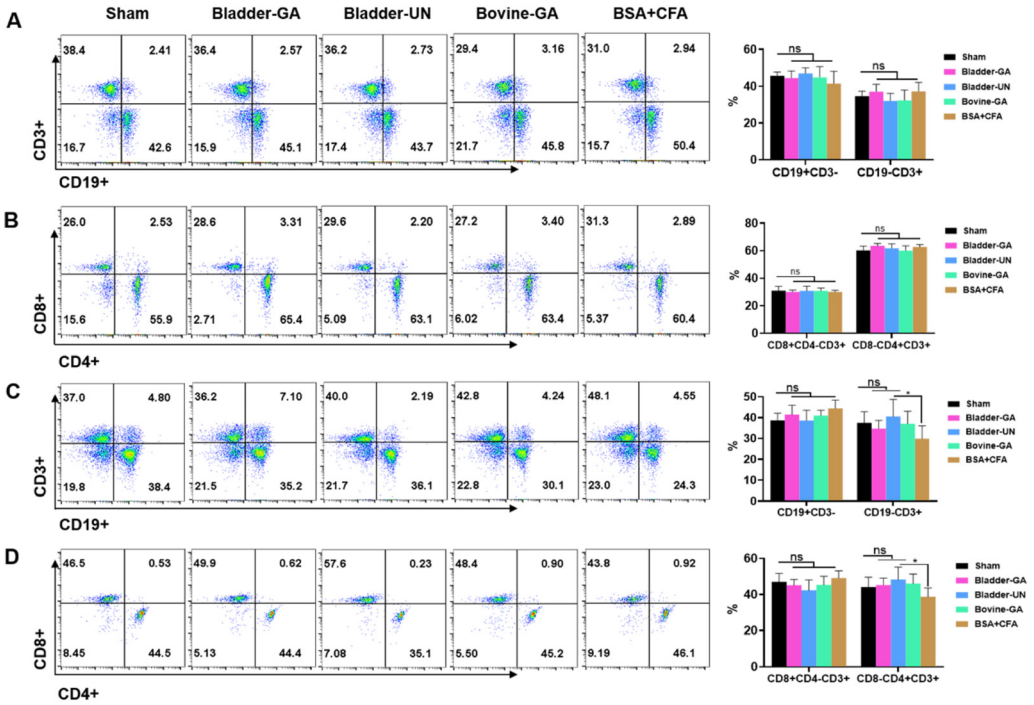

Fig. 4 Flow cytometry for lymphocytes after implantation for 7 days and 30 days. CD3+, CD19+, CD3+CD8+, and CD3+CD4+ represent T lymphocyte, B lymphocyte, CD8+T lymphocyte and CD4+T lymphocyte in spleen. The proportions of CD3+, CD19+, CD3+CD8+ and CD3+CD4+ were stable after implantation for 7 days (A and B) and 30 days (C and D). ns = non-significant, n = 6.

3.5 Blood routine examination and cytokines

C-Reactive protein (CRP) levels were higher in each group at 3 days and decreased at 7 days after implantation but slightly increased at day 30. The CRP concentrations of Bladder-GA and Bladder-UN showed no obvious change compared with the sham group. Routine blood examination results at 3, 7, and 30 days after subcutaneous implantation are shown in the ESI (Fig. S1†). Cytokines IL-1β, TNF-α, IFN-γ, IL-6, IL-12P70, and CRP can react to inflammation, while IL-4 and IL-10 can inhibit inflammation. The results showed that there was no difference in the levels of IL-1 β, IFN-γ, and IL-6 between the Bladder-GA, Bladder-UN, and sham groups at 3, 7, and 30 days, and there was no significant difference in the levels of TNF-α between the Bladder-GA, Bladder-UN, Bovine-GA, and sham groups at 3 and 7 days, while the TNF-α level of Bladder-GA increased slightly after 30 days of subcutaneous implantation. The IL-6 levels in both the Bladder-GA and Bladder-UN groups were lower than those in the Bovine-GA group at 3, 7, and 30 days. The concentrations of IL-4 and IL-10 were not significantly different from those of the sham group over the entire implantation period. IL-5 and IL-2 concentrations in Bladder-GA and Bladder-UN groups showed no obvious change compared to the sham group at 3, 7, and 30 days after implantation (Fig. 5).

3.6 H&E staining and macrophages at the implantation site

The materials at 7 and 30 days were removed to observe the local pathological conditions. It could be seen that there were a few inflammatory cells, no tissue necrosis, fiber wrapping and granulation tissue near the material of Bovine-GA. There was no obvious infiltration of inflammatory cells in the

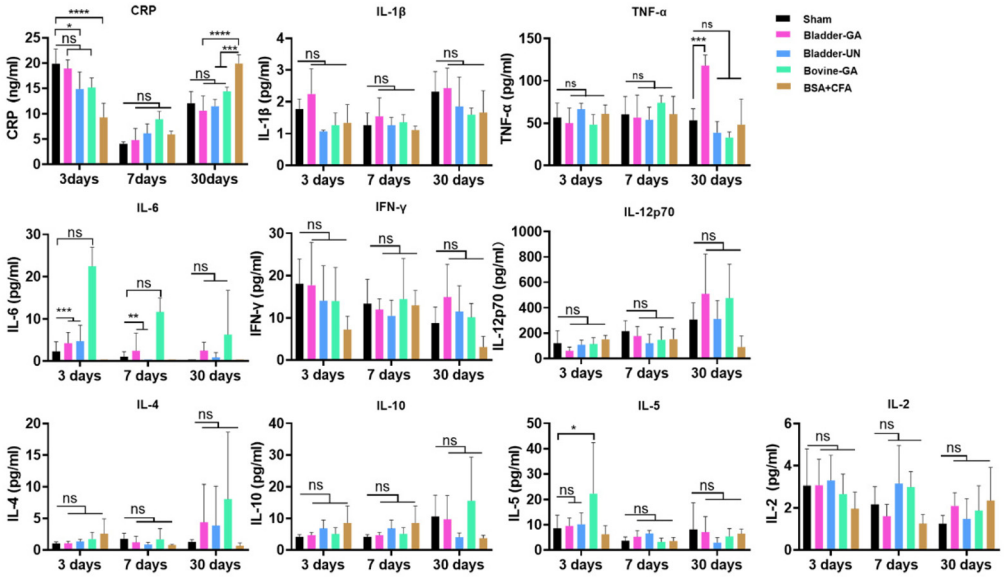

Fig. 5 C-Reactive protein (CRP) is an acute protein produced when the body is exposed to foreign grafts, and the content changes with the time of transplantation, showing the highest level at the beginning of implantation. IL-6, IL-12p70, IFN-γ, TNF-α and IL-1β represent the pro-inflammatory factors, and IL-4 and IL-10 are anti-inflammatory factors. IL-2 and IL-5 increase if there are immune rejections after transplantation. *$p < 0.05$, **$p < 0.01$, ***$p < 0.001$ and ****$p < 0.0001$, ns = non-significant, $n = 4$.

Bladder-GA group at 7 and 30 days, and there was less infiltration than that in the Bladder-UN group, and angiogenesis was observed at day 30. Cell infiltration of Bladder-UN at 30 days was greater than that at 7 days. We found no serious inflammatory reactions, such as granulomatous fibrosis, at the implantation site at 7 or 30 days (Fig. 6 and 8A).

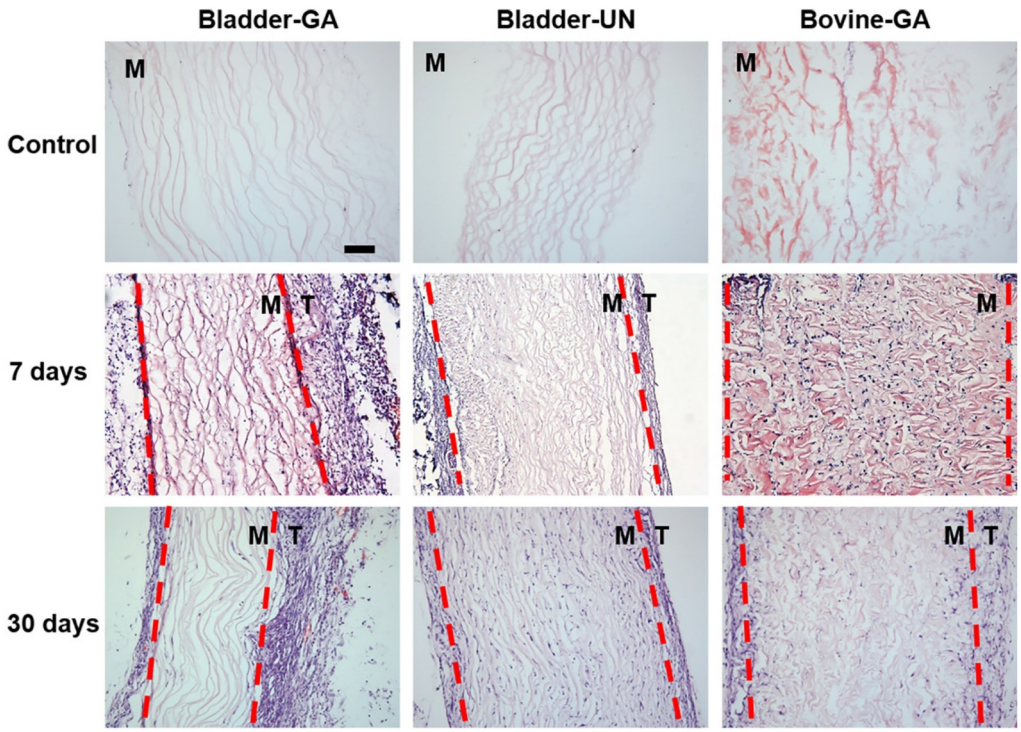

Fig. 6 H&E staining of the materials at 7 days and 30 days after implantation. The infiltration of cells into the material and whether there were abnormal manifestations in the attached tissue were observed, T: tissue and M: material; scale bar is 100 μm. Tissue and material are distinguished by the red dashed line; T: tissue and M: material.

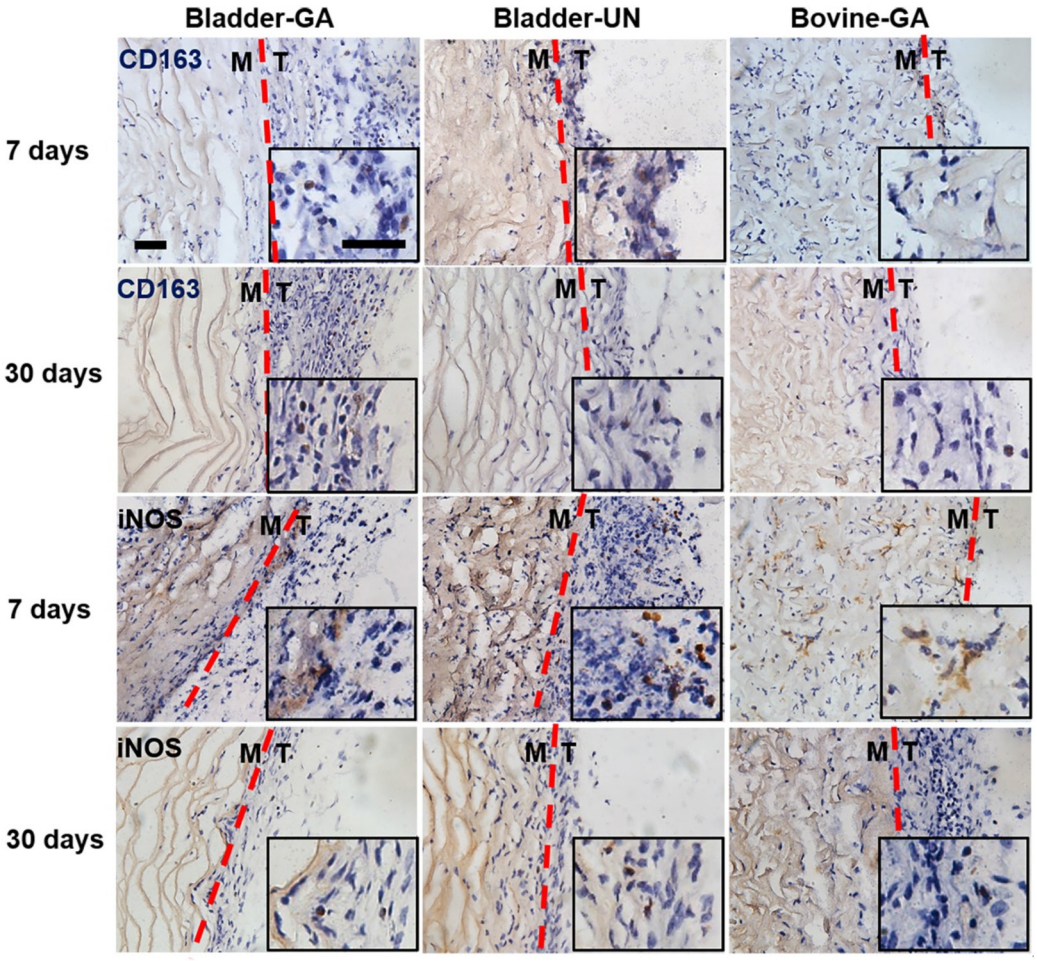

Fig. 7 Distribution of M1 and M2 in subcutaneous implantation sites at 7 days and 30 days. iNOS represented type M1 macrophages and CD163 represented type M2 macrophages; the scale bar is 50 μm. Tissue and material are distinguished by the red dashed line, T: tissue, M: material.

More CD163+ macrophages were detected in Bladder -GA and Bladder-UN groups at 7 days (Fig. 7). There were more iNOS cells at 7 days and more CD163+ cells in the Bovine-GA group at 30 days. More CD163+ macrophages were present in Bladder-GA than in Bovine-GA, and the proportion of CD163+/iNOS macrophages in Bladder-GA was further verified (Fig. 8B).

3.7 Histopathology and apoptosis of various organs

After subcutaneous implantation, it could be seen that there were no obvious pathological changes and inflammatory cell infiltration in the heart, liver, lung, kidney and thymus organs of each group at 7 days and 30 days (Fig. 9 and Fig. S2†), and

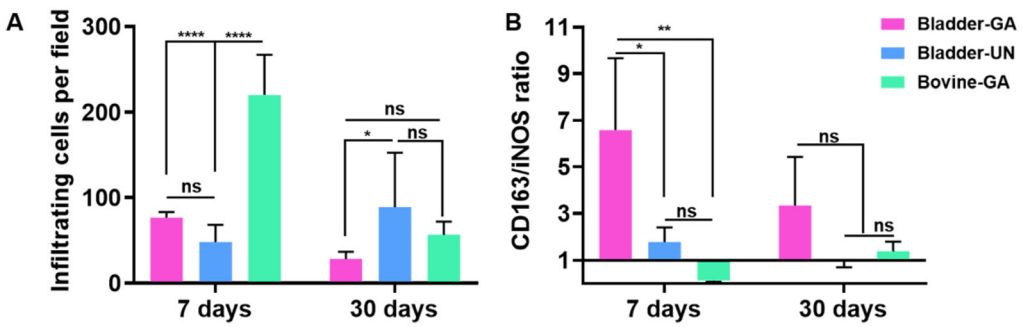

Fig. 8 (A) Cellular infiltration statistics from H&E staining of the materials at 7 days and 30 days after implantation. (B) CD163/iNOS macrophage proportion was calculated from the images of distribution of M1 and M2 in subcutaneous implantation sites at 7 days and 30 days. *$p < 0.05$, **$p < 0.01$ and ns = non-significant, $n = 4$.

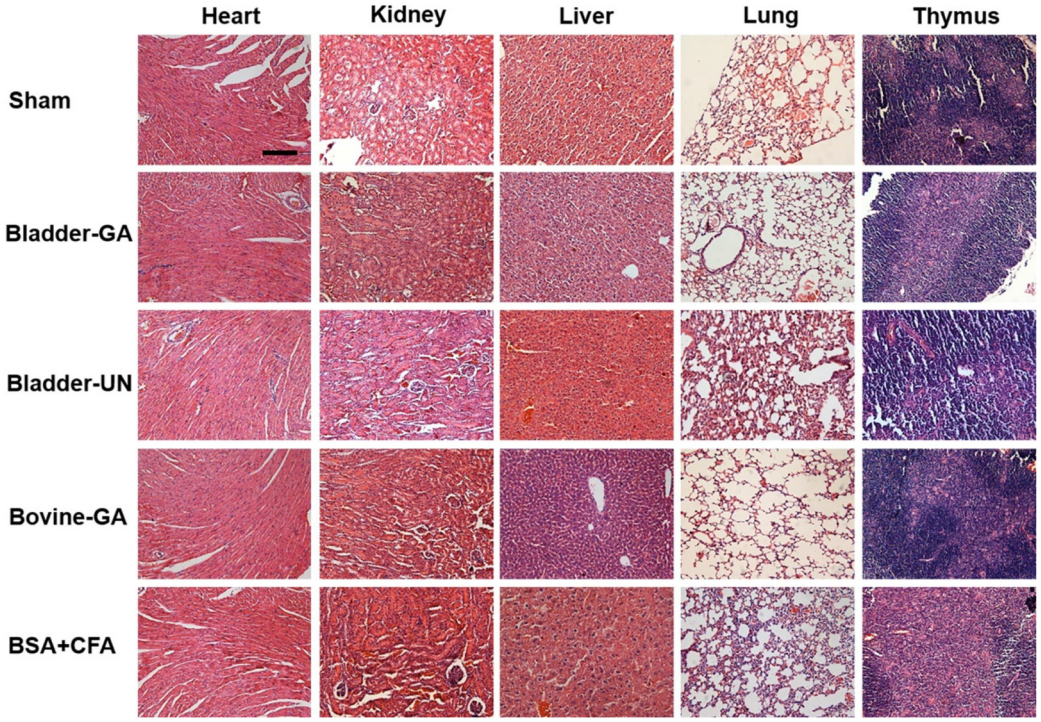

Fig. 9 The histopathology of the heart, liver, lungs, and thymus explanted from mice after 7 days of implantation; the scale bar is 200 μm.

no obvious apoptotic cells were observed in the TUNEL staining results (Fig. 10 and Fig. S3†).

4. Discussion

Swim bladder-derived biomaterials have the advantages of anti-calcification, adequate mechanical properties, and good biocompatibility, and are promising alternatives as cardiovascular materials. To facilitate the clinical application of these novel biomaterials, immunogenic safety is the primary evaluation criterion, and should be carefully evaluated at the initial stage of development. Understanding their immune response *in vivo* will help evaluate their potential acceptance in humans and provide important predictors for early intervention of local or systemic immune responses during application. In this study, we assessed the immunogenicity of glutaraldehyde crosslinked bladders (Bladder-GA) and un-crosslinked bladders (Bladder-UN) using *in vitro* and *in vivo* assays, according to ISO 10993-20. This study gives important evidence that swim bladder-derived materials did not elicit significant aberrant immune responses *in vivo.*

As animal-derived materials, the immunogenic safety of swim bladder-derived biomaterials is one major concern for realizing their clinical applications, which may be elicited by residual tissue proteins, nucleic acids, antigens and other substances due to the preparation process.[18] Xenograft rejection of transplanted materials or medical devices usually leads to graft non-function or body damage, which determines the success or failure of clinical transplantation.[19] The innate immune response occurs immediately[20] by the activation of innate immune cells and secretion of multiple cytokines to remove pathogens and foreign bodies.[21] C-Reactive protein (CRP) is a well-known acute immune protein, which rises sharply in serum when the body is infected or damaged, subsequently activating the complement and strengthening the phagocytosis of phagocytes to remove invading pathogenic microorganisms or injured cells.[22,23] As shown in Fig. 5, we found that the serum CRP level was the highest at day 3 and then decreased at day 7 in all groups except the BSA-treated group. These values were slightly lower in the bladder groups than in the sham group. We speculate that the high CRP level was mainly due to the surgical procedure, rather than the implanted biomaterials. Meanwhile, the pro-inflammatory factors, such as IL-6, IL-12p70, IFN-γ, TNF-α, and IL-1β, were steady in both the bladder groups at all the determined time points, and the levels were very close to those in the sham group. Anti-inflammatory factors, such as IL-4 and IL-10, were the highest at long-term post-implantation, which was reasonable as a physiological repair process after injury. As reported, the levels of IL-6 and IL-5 increase significantly in the presence of immune rejection after renal transplantation in human.[24] Unexpectedly, they were obviously higher in the Bovine-GA group than in both bladder groups and the sham group at 3 days. However, the former has been widely used as a heart valve substitute in clinics for a long time.

Adaptive immune responses are usually activated after the acute immune stage. Among them, the effect of biomaterials

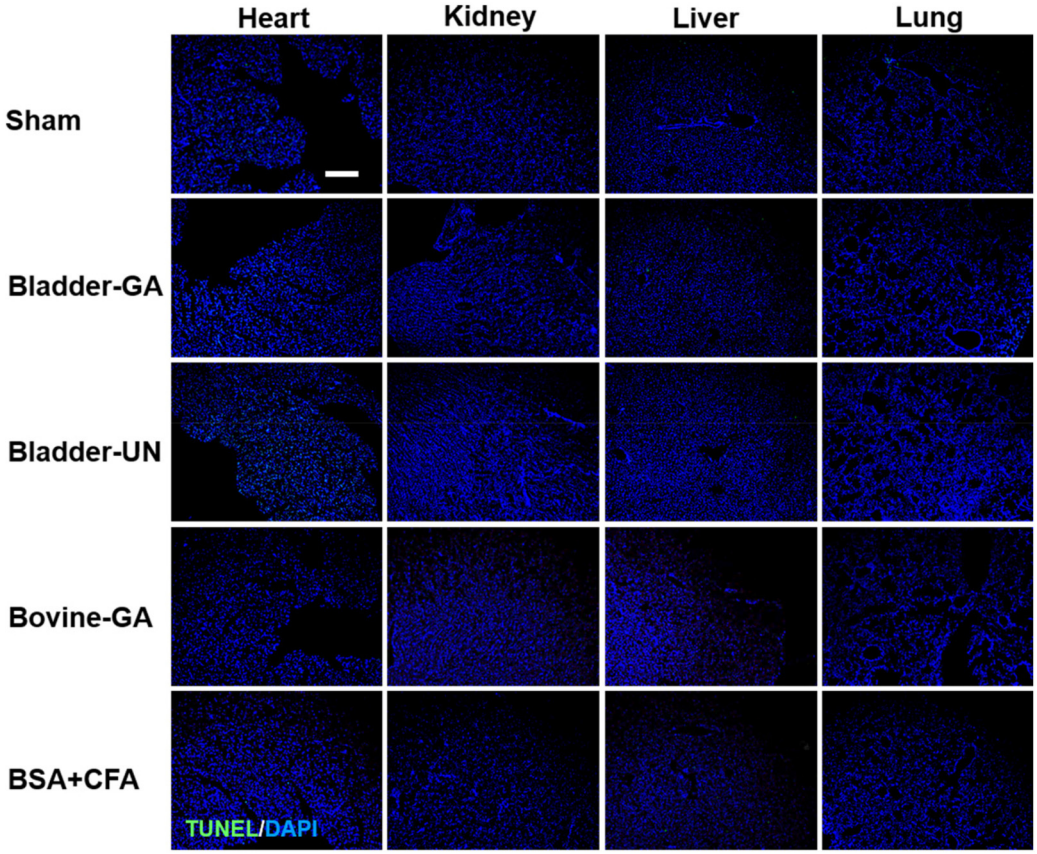

Fig. 10 The apoptosis of the heart, liver, lungs, and thymus explanted from mice after 7 days of implantation (TUNEL, green and DAPI, blue); the scale bar is 200 μm.

on lymphocyte proliferation could identify directly whether it affects immune function.[25] In this study, we found no significant difference in lymphocyte proliferation between the swim bladder and sham groups in both *in vitro* and *in vivo* implantation at 7 and 30 days, as shown in Fig. 1. In addition, as shown in Fig. 2 and 4, the thymus coefficient, spleen coefficient and ratio of immune cell subtypes CD19+, CD3+CD8+, and CD3+CD4+ cells showed no significant differences between the bladder and sham groups at 7 and 30 days after implantation. In addition, Lu *et al.* reported the humoral immune response caused by antigens from xenografts as a substantial factor in stimulating severe organ immune rejection in clinical trials.[26] The serum immunoglobulin level can indicate whether humoral immunity occurs post-implantation. IgM antibodies are usually produced at the early stage post-implantation and have strong cytotoxic and cytolytic activities.[27,28] In addition, IgG antibodies are usually produced several weeks after a stimulus to activate complements and neutralize a series of antigens in the immune response. In the field of xenograft transplantation, α-Gal[29] and anti-Neu5Gc[30] have been widely proven to be the main antigens that cause immune resistance in organs. As shown in Fig. 3B, the total IgG levels in Bladder-GA and Bladder-UN groups were very close to those in the sham group at 30 days post-implantation, indicating that no obvious humoral immune response was elicited by bladder biomaterials. This result may be due to the absence of α-Gal and Neu5Gc expression in fish. In summary, these results indicate that the swim bladder material does not induce strong cellular or humoral immune responses in mice.

The foreign body response to biomaterials usually occurs at the implant site with prolonged pro-inflammatory activity. Pro-inflammatory reactions, M1 cell activation, formation of multinucleated foreign body giant cells and granulomatous inflammation eventually interfere with the mechanical properties of the material and lead to material destruction[31,32] characterized adverse chronic reaction. As seen in Fig. 6 and 8, H&E staining showed that there was no obvious inflammatory reaction such as granuloma and fibrosis in the implanted site of swim bladder biomaterials at 7 and 30 days after implantation, and Bladder-GA was dominated by M2 macrophages, which indicated beneficial constructive remodeling. Similarly, the chronic outcome after transplantation is primarily material remodeling, including alternate activation of M2 macrophages,[31] production of a new matrix, and their subsequent differentiation into a valvular mesenchymal phenotype.[14]

The fish swim bladder showed a superior anti-calcification property, but the mechanism is not clear. As is known, pros-

thetic valve calcification has three common reasons. One is tearing of the valve caused by long-term opening and closing, and the second is the remaining aldehyde group on the leaflet after glutaraldehyde crosslinking. Additionally, inflammation and immune rejection can also cause severe calcification. One recent study[16] discovered that α-gal and Neu5Gc, as two main antigens unique to mammals, can cause long-term rejection reactions, including calcification and failure of the valve leaflets after implantation. This finding provides a key explanation for why bioprosthetic valve materials from porcine and bovine tissues are calcified in clinical practice. Fish from which swim bladders were taken were not mammal species and lacked α-gal and Neu5Gc antigens. Combined with the results of this study, we consider that the low immunogenicity of fish swim bladders contributes to their superior anti-calcification property.

There are some limitations of this study. The results were obtained from a small number of experimental animals. As is known, the immune response in small animal models is not exactly the same as that in humans, and further assessments in large animal models or humans is necessary. In addition, potential antigens which may cause allergy or rejection should be further carefully assessed.

5. Conclusion

Herein, the immunogenic safety of fish swim bladder-derived biomaterials was assessed using *in vitro* and *in vivo* assays. The data proved that the function of immune organs and immune cells was not activated by the swim bladder, in terms of the thymus coefficient, spleen coefficient, immune cell subtypes, and splenocyte proliferation. In addition, the IgG content in the serum of the swim bladder group was close to that of the sham group, indicating that no obvious humoral immune responses were induced. Importantly, no encapsulation due to foreign body reaction was found around the implant; however, it was surrounded by more M2 macrophages. Overall, the swim bladder-derived material did not elicit significant aberrant immune responses *in vivo*, giving enough confidence for its use in tissue engineering or medical devices.

Abbreviations

Bladder-GA	Glutaraldehyde crosslinked fish swim bladder
Bladder-UN	Un-crosslinked swim bladder
Bovine-GA	Glutaraldehyde crosslinked bovine pericardium
VHDs	Valvular heart diseases
BHVs	Bioprosthetic heart valves
TAVR	Transcatheter aortic valve replacement
SDVGs	Small diameter vascular grafts
α-gal	Carbohydrate epitope α-1,3-galactose
Neu5Gc	*N*-Glycolylneuraminic acid
CRP	C-reactive protein
LPS	Lipopolysaccharide
ConA	Concanavalin A
CFA	Complete Freund's adjuvant
BSA	Bovine serum albumin

Conflicts of interest

There is no conflict to declare.

Acknowledgements

This work was financially supported by the Natural Science Foundation of China (no. 32071356 and 82272158), CAMS Innovation Fund for Medical Sciences (2022-I2M-1-023), Natural Science Fund for Distinguished Young Scholars of Tianjin (22JCJQJC00110), Fundamental Research Funds for the Central Universities (3332022069), and Open Fund of Tianjin Enterprise Key Laboratory of Hyaluronic Acid Application Research (KTRDHA-Z201902) provided by Tianjin Kangting Bioengineering Group Corp. L.T.D.

References

1 A. Sanaani, S. Yandrapalli and J. M. Harburger, *Cardiol. Rev.*, 2018, **26**, 177–186.
2 S. Coffey, R. Roberts-Thomson, A. Brown, J. Carapetis, M. Chen, M. Enriquez-Sarano, L. Zühlke and B. D. Prendergast, *Nat. Rev. Cardiol.*, 2021, **18**, 853–864.
3 S. Coffey, B. J. Cairns and B. Iung, *Heart*, 2016, **102**, 75–85.
4 C. M. Cunanan, C. M. Cabiling, T. T. Dinh, S. Shen, P. Tran-hata, J. H. R. Iii, M. C. Fishbein, E. Lifesciences and L. L. C. Crystal, *Control*, 2001, **4975**, S417–S421.
5 S. V. Arnold, M. R. Reynolds, K. Wang, E. A. Magnuson, S. J. Baron, K. M. Chinnakondepalli, M. J. Reardon, P. N. Tadros, G. L. Zorn, B. Maini, M. A. Mumtaz, J. M. Brown, R. M. Kipperman, D. H. Adams, J. J. Popma and D. J. Cohen, *JACC: Cardiovasc. Interventions*, 2015, **8**, 1207–1217.
6 C. Yerasi, T. Rogers, B. J. Forrestal, B. C. Case, J. M. Khan, I. Ben-Dor, L. F. Satler, H. M. Garcia-Garcia, J. E. Cohen, H. Kitahara, C. Shults and R. Waksman, *JACC: Cardiovasc. Interventions*, 2021, **14**, 1169–1180.
7 A. Koziarz, A. Makhdoum, J. Butany, M. Ouzounian and J. Chung, *Curr. Opin. Cardiol.*, 2020, **35**, 123–132.
8 J. Liu, B. Li, H. Jing, Y. Wu, D. Kong, X. Leng and Z. Wang, *Adv. Healthcare Mater.*, 2020, **9**, 1–13.
9 B. Li, H. Jing, Z. Sun, X. Wang, D. Kong, J. Liu, X. Leng and Z. Wang, *Smart Mater. Med.*, 2021, **2**, 209–218.
10 N. Li, X. Li, Y. Ma, F. Qiao, Y. Bai, X. Liu and Z. Xu, *Biomater. Sci.*, 2021, **9**, 8356–8365.
11 H. Bai, P. Sun, H. Wu, S. Wei, B. Xie, W. Wang, Y. Hou, J. Li, A. Dardik and Z. Li, *Commun. Biol.*, 2021, **4**, 1–11.
12 M. Nurilmala, N. Darmawan, E. A. W. Putri, A. M. Jacoeb and T. T. Irawadi, *Int. J. Biomater.*, 2021, **2021**, 6658002.

13 Q. Li, F. Zhang, H. Wang and T. Pan, *Neurol. Res.*, 2019, **41**, 242–249.
14 M. Ground, S. Waqanivavalagi, R. Walker, P. Milsom and J. Cornish, *Acta Biomater.*, 2021, **133**, 102–113.
15 S. J. Bozso, R. El-Andari, D. Al-Adra, M. C. Moon, D. H. Freed, J. Nagendran and J. Nagendran, *Scand. J. Immunol.*, 2021, **93**, 1–7.
16 T. Senage, A. Paul, T. Le Tourneau, I. Fellah-Hebia, M. Vadori, S. Bashir, M. Galiñanes, T. Bottio, V. Padler-Karavani, *et al.*, *Nat. Med.*, 2022, **28**, 283–294.
17 ISO 10993-20, Biological evaluation of medical devices-Part 20: Principles and methods for immunotoxicology testing of medical devices.
18 A. L. Predeina, M. S. Dukhinova and V. V. Vinogradov, *J. Mater. Chem. B*, 2020, **8**, 10010–10022.
19 K. L. O'Keefe, S. D. Cohle, J. E. McNamara and R. L. Hooker, *Ann. Thorac. Surg.*, 2011, **91**, 1269–1272.
20 R. A. Manji, W. Lee and D. K. C. Cooper, *Int. J. Surg.*, 2015, **23**, 280–284.
21 H. Huang, Y. Lu, T. Zhou, G. Gu and Q. Xia, *Front. Immunol.*, 2018, **9**, 1–8.
22 M. Löbler, M. Sa, C. Kunze, K. P. Schmitz and U. T. Hopt, *J. Biomed. Mater. Res.*, 2002, **61**, 165–167.
23 D. Iglesias-Álvarez, D. López-Otero, R. González-Ferreiro, X. Sanmartín-Pena, B. Cid-Álvarez, R. Trillo-Nouche and J. R. González-Juanatey, *Circ.: Cardiovasc. Interventions*, 2018, **11**, 1–3.
24 K. Doberer, M. Duerr, P. F. Halloran, F. Eskandary, K. Budde, H. Regele, J. Reeve, A. Borski, N. Kozakowski, R. Reindl-Schwaighofer, J. Waiser, N. Lachmann, S. Schranz, C. Firbas, J. Mühlbacher, G. Gelbenegger, T. Perkmann, M. Wahrmann, A. Kainz, R. Ristl, F. Halleck, G. Bond, E. Chong, B. Jilma and G. A. Böhmig, *J. Am. Soc. Nephrol.*, 2021, **32**, 708–722.
25 J. Muhamed, D. Revi, A. Rajan, S. Geetha and T. V. Anilkumar, *Toxicol. Pathol.*, 2015, **43**, 536–545.
26 T. Lu, B. Yang, R. Wang and C. Qin, *Front. Immunol.*, 2020, **10**(3060).
27 W. Wang, L. Zhang, L. Sun, Z. D. She, R. W. Tan and X. F. Niu, *Biomed. Environ. Sci.*, 2018, **31**, 829–842.
28 L. You, X. Weikang, Y. Lifeng, L. Changyan, L. Yongliang, W. Xiaohui and X. Bin, *Artif. Cells, Nanomed., Biotechnol.*, 2018, **46**, 334–344.
29 G. Huai, P. Qi, H. Yang and Y. Wang, *Int. J. Mol. Med.*, 2016, **37**, 11–20.
30 S. A. Springer, S. L. Diaz and P. Gagneux, *Immunogenetics*, 2014, **66**, 671–674.
31 S. F. Badylak, *Ann. Biomed. Eng.*, 2014, **42**, 1517–1527.
32 A. Costa-Pinto, T. C. Santos, N. M. Neves and R. L. Reis, *Biomater. Nat. Adv. Devices Ther.*, 2016, 562–579.